

UC Berkeley

UC Berkeley Previously Published Works

Title

The effects of post-growth annealing on the structural and magnetic properties of BaFe₂As₂

Permalink

<https://escholarship.org/uc/item/6kj7z7pp>

Journal

Journal of Physics Condensed Matter, 28(11)

ISSN

0953-8984

Authors

Forrest, TR
Valdivia, PN
Rotundu, CR
et al.

Publication Date

2016-03-23

DOI

10.1088/0953-8984/28/11/115702

Peer reviewed

PAPER

The effects of post-growth annealing on the structural and magnetic properties of BaFe_2As_2

To cite this article: T R Forrest *et al* 2016 *J. Phys.: Condens. Matter* **28** 115702

View the [article online](#) for updates and enhancements.

Related content

- [The growth of 122 and 11 iron-based superconductor single crystals and the influence of doping](#)
D P Chen and C T Lin
- [Europium-based iron pnictides: a unique laboratory for magnetism, superconductivity and structural effects](#)
Sina Zapf and Martin Dressel
- [Nematicity, magnetism and superconductivity in FeSe](#)
Anna E Böhmer and Andreas Kreisel



IOP | ebooks™

Bringing you innovative digital publishing with leading voices to create your essential collection of books in STEM research.

Start exploring the collection - download the first chapter of every title for free.

The effects of post-growth annealing on the structural and magnetic properties of BaFe_2As_2

T R Forrest,^{1,5} P N Valdivia², C R Rotundu,^{3,6} E Bourret-Courchesne⁴
and R J Birgeneau^{1,2,3}

¹ Department of Physics, University of California, Berkeley, CA 94720, USA

² Department of Materials Science and Engineering, University of California, Berkeley, CA 94720, USA

³ Materials Sciences Division, Lawrence Berkeley National Laboratory, Berkeley, CA 94720, USA

⁴ Life Sciences Division, Lawrence Berkeley National Laboratory, Berkeley, CA 94720, USA

E-mail: forrest@esrf.fr

Received 7 October 2015, revised 18 December 2015

Accepted for publication 25 January 2016

Published 19 February 2016



Abstract

We investigate the effects of post-growth annealing on the structural and magnetic properties of BaFe_2As_2 . Magnetic susceptibility measurements, which exhibit a signal corresponding to the magnetic phase transition, and high-resolution x-ray diffraction measurements, which directly probe the structural order parameter, show that annealing causes the ordering temperatures of both the phase transitions to increase, sharpen and converge. In the as grown sample, our measurements show two distinct transitions corresponding to structural and magnetic ordering, which are separated in temperature by approximately 1 K. After 46 days (d) of annealing at 700 °C, the two become concurrent in temperature. These measurements demonstrate that the structural phase transition is second-order like when the magnetic and structural phase transitions are separated in temperature, and first-order like when the two phase transition temperatures coincide. This observation indicates that annealing causes the system to cross a hitherto undiscovered tricritical point. In addition, x-ray diffraction measurements show that the *c*-axis lattice parameter increases with annealing up to 30 d, but remains constant for longer annealing times. Comparisons of BaFe_2As_2 to SrFe_2As_2 are made when possible.

Keywords: iron-pnictide superconductors, structural phase transition, annealing

(Some figures may appear in colour only in the online journal)

1. Introduction

The discovery of high-temperature superconductivity in the layered iron-pnictide materials [1] has generated great excitement within the strongly correlated electron community. While research into the pnictides is still ongoing, one of the central results has been the intimate connection between

superconductivity, magnetism and the lattice structure. Thus to explain how superconductivity emerges in these materials, one must understand the interaction between these three degrees of freedom. To date superconductivity has been identified in several groups of pnictides which have related structures [1–4]. For the majority of these systems, the parent compounds exhibit a spin-density wave antiferromagnetic order at low temperatures, although there are some exceptions [3, 4]. In most cases the magnetic ordering is either preceded or accompanied by a structural phase transition, where the crystal lattice changes from a high temperature tetragonal to a low temperature orthorhombic structure. Upon chemical

⁵ Present address: European Synchrotron Radiation Facility, BP 220, F-38043 Grenoble Cedex, France

⁶ Present address: Stanford Institute for Materials and Energy Sciences, SLAC National Accelerator Laboratory, 2575 Sand Hill Road, Menlo Park, CA 94025, USA

substitution the ordering temperatures of both transitions are suppressed, and in some cases superconductivity is induced. The archetypal class of pnictide superconductors are derived from parent compounds with the chemical formula: $M\text{Fe}_2\text{As}_2$ ($M = \text{Ca}, \text{Sr}, \text{Ba}$), and are commonly known as the 122 compounds. For this structural class, superconductivity has been identified with substitution on all three atomic sites [2, 5–9], or through the application of hydrostatic pressure [10, 11]. In addition, superconductivity has also been induced by the application of epitaxial strain in thin films of BaFe_2As_2 [12]. There has already been a significant amount of research conducted into the nature of the structural and magnetic phase transitions in these compounds. For CaFe_2As_2 and SrFe_2As_2 , the consensus is that the phase transitions are concurrent in temperature, and can therefore be thought of as a single first-order magnetostructural transition [13–15]. The case of BaFe_2As_2 is more complex however; there have been reports of these phase transitions being both first [16] and second-order, or at least nearly so [17]. Of particular relevance is the previous research conducted by the authors of this paper [18], where high resolution heat capacity, resistivity and x-ray diffraction measurements were taken on a BaFe_2As_2 single crystal, that had been wrapped in tantalum foil and annealed in a low pressure argon atmosphere at 700 °C. Results showed that anomalies observed in the resistivity and heat capacity were raised in temperature from 135.4 K to 140.2 K after 30 d of annealing. Measurements of the sample’s residual resistivity ratio (RRR) showed a consistent improvement with annealing time. This result was confirmed by a later work where BaFe_2As_2 single crystals were annealed in a BaAs powder [19]. Returning to our previous research [18], heat capacity measurements on the as grown sample showed a peak in C/T that is consistent with a first-order transition. Furthermore, the 30 d of annealing caused the peak to increase and sharpen in temperature. To corroborate this interpretation, high resolution x-ray diffraction measurements of the structural phase transition were performed on the sample after 30 d of annealing. The x-ray measurements showed that upon cooling the orthorhombic distortion initially appeared as a continuous splitting of the tetragonal reflection. At a slightly lower temperature this continuous splitting was interrupted by the abrupt appearance of a second set of orthorhombic reflections, whose positions remain approximately constant. As the sample was cooled further, the first set of reflections were rapidly suppressed; their positions continued to move outwards, but never merged with the second set of reflections. This important result suggests that the structural phase transition in 30 d annealed BaFe_2As_2 begins as second-order, but evolves into a first-order transition upon lowering of the temperature. It was speculated that the driving force behind this evolution is the formation of the antiferromagnetic order [18]. This unusual structural phase transition was confirmed in an as grown sample of BaFe_2As_2 by Kim *et al* [20], who also conclusively showed that the discontinuous jump in the structural phase transition’s order parameter does indeed correspond to the appearance of the antiferromagnetic order. Thus over a small temperature range it is

proposed that BaFe_2As_2 exists in a phase which has an orthorhombic structure, but is paramagnetic. Furthermore, Kim *et al* performed similar x-ray measurements of the structural order parameter in $\text{Ba}(\text{Fe}_{1-x}\text{Co}_x)_2\text{As}_2$ and $\text{Ba}(\text{Fe}_{1-x}\text{Rh}_x)_2\text{As}_2$. For the Co-substituted compound, a tricritical point wherein the two phase transitions become completely separated and the magnetic phase transition becomes second-order, was identified at a doping level of $x \approx 0.22$. This result was later confirmed by separate resistivity measurements [21].

There is therefore a subtle difference in the structural and magnetic ordering temperatures in BaFe_2As_2 , although they are still strongly coupled to one another. This has been demonstrated by mean-field calculations of the free energy, which show that the structural phase transition is not due to an intrinsic structural instability, but instead arises from magnetoelastic coupling to an Ising-nematic degree of freedom of the magnetic ground states [20]. What is more, the inclusion of an anharmonic term to the elastic free energy was shown to reproduce the phase diagram of $\text{Ba}(\text{Fe}_{1-x}\text{Co}_x)_2\text{As}_2$ by solely changing the material’s elastic properties. Specifically, an increase in the bare shear modulus leads to a suppression of the two phase transition temperatures and causes them to diverge. Initially the structural transition is second-order and the magnetic transition is first-order, with its onset causing the discontinuity in the structural order parameter. Upon a further increase of the bare shear modulus, the magnetic transition also becomes second-order, creating a tricritical point. Interestingly, the model also predicts that reducing shear modulus will cause the two phase transitions to increase in temperature, finally becoming concurrent and first-order [20]. Since annealing offers a clean method to change the structural and magnetic ordering temperatures, and possibly their separation, it affords a good opportunity to search for changes in the coupling between the two phase transitions. Furthermore, it is important to study the limiting behaviour of extended annealing periods, as it might allow for the access of regions of the BaFe_2As_2 phase diagram that have not yet been measured.

In addition, while it has been shown that annealing has a substantial effect on the structural and magnetic ordering in BaFe_2As_2 , it is still not understood what effect it has at the microscopic level. For example, is the main effect of annealing to remove defects and other impurities which act as a chemical dopant? Or does annealing cause changes in the effective pressure within the crystal?

In order to answer these questions, we have undertaken a number of x-ray diffraction and magnetic susceptibility measurements on a single crystal of BaFe_2As_2 that was annealed for a cumulative period of 46 d. In addition, high resolution x-ray diffraction measurements of the structural phase transition in as grown, and after 30 and 46 d of annealing were also taken. Since neutron diffraction is unable to resolve the jump in the structural phase transition [17], these high resolution x-ray diffraction measurements offer a method to accurately determine the separation in ordering temperatures. A full description of these measurements is given in section 2, while the experimental results are shown in section 3. Finally this work is discussed in section 4, and the conclusions are given in section 5.

2. Experimental details

A single crystal of BaFe_2As_2 was grown using the self-flux method [22]. In order to prevent the absorption of oxygen during the annealing process, the crystal was wrapped in tantalum foil (a getter that readily combines with oxygen), and placed inside a quartz tube that was filled with argon gas. The tube was then evacuated using a combined roughing and turbo pump set-up. The pumping was continued until a pressure level of less than 1×10^{-5} mbar was displayed, after which the tube was immediately sealed. The sample was then annealed at 700 °C for cumulative periods of 22, 30 and 46 d. X-ray diffraction measurements of the room temperature lattice parameters, and magnetic susceptibility measurements of the phase transition(s), were taken on the sample as grown and after each annealing period. The magnetic susceptibility measurements were taken with a Quantum Design Magnetic Property Measurement System (MPMS), with a magnetic induction of 5T, parallel to the sample's a-b crystallographic plane. The susceptibility was recorded upon cooling through the phases transition(s) at intervals of 0.25 K. The x-ray diffraction measurements of the (0 0 4), (0 0 8) and (0 0 12) reflections were taken using a X'Pert pro four-circle diffractometer, with a monochromated $\text{Cu-}\alpha_1$ source. High resolution x-ray diffraction measurements of the structural phase transition were taken at beamline 7-2, Stanford Synchrotron Radiation Laboratory, on the sample as grown and after 30 and 46 d of annealing. The diffraction measurements were taken with an x-ray photon energy of 16 keV, in a vertical scattering geometry. Transverse scans (rocking curves) of the (0 0 8) reflection in as grown and after 30 d of annealing, gave a full width at half maximum (FWHM) in θ of $\leq 0.1^\circ$, indicating a good quality of the surface mosaic. Transverse scans (rocking curves) of the same reflection after 46 d of annealing gave a FWHM of $\sim 0.25^\circ$. In order to study the structural phase transition, high resolution reciprocal space scans along the [1 1 0] direction were used to measure the splitting of an (H H L) tetragonal reflection into the (H 0 L) and (0 H L) orthorhombic reflections. (It was not possible to measure the splitting of a (H H 0) reflection as the crystal natural cleaves with the [0 0 1] direction as the surface normal.) For the as grown and 30 d annealed samples, the splitting of the $(3\ 3\ 18)_T$ reflection was measured. For the 46 d annealed sample, scans along the [1 1 0] direction across $(3\ 3\ 18)_T$ reflection did not show a clean single peak in the tetragonal phase. Since this scan is not completely perpendicular to the crystal mosaic arc, it is likely that the degradation in crystal mosaic quality of the 46 d annealed sample is responsible for this effect. By contrast the $(2\ 2\ 16)_T$ reflection, where the [1 1 0] reciprocal lattice scan is more perpendicular to the crystal mosaic arc, showed single peak in the tetragonal phase. Therefore the splitting of this reflection was measured in the 46 d annealed sample. It should be noted that previous measurements of the structural phase transition in BaFe_2As_2 studied the splitting of (2 2 L) or (1 1 L) type reflections [18, 20]. Therefore measurements on the (2 2 16) will still be able to resolve the unusual splitting of the peak, if it is present. These reciprocal lattice scans were taken as the temperature was decreased from 160 K to a base

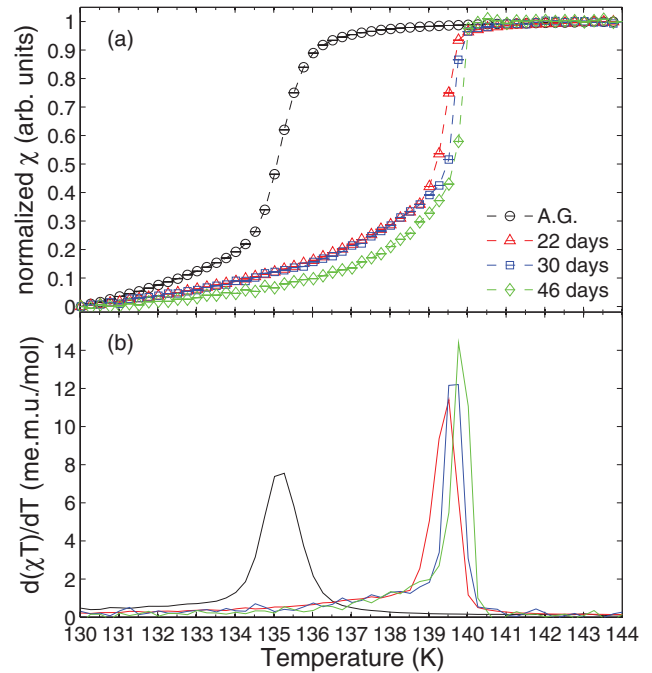


Figure 1. (a) χ versus T of the phase transitions for a BaFe_2As_2 sample, as grown and after 22, 30 and 46 d of annealing. The data has been normalized to be 0 at 130 K and 1 at 145 K. (b) $\partial(\chi T)/\partial(T)$ versus T .

temperature of 80 K. Close to the structural phase transition, measurements were taken at temperature steps of 0.1 K. A rest period of at least 4 min preceded each scan, this ensured that the measured temperature fluctuations were less than 0.025 K.

3. Experimental results

The process of annealing causes the crystals to dull. To determine if this effect is indicative of a change in chemical composition, wavelength dispersive x-ray spectroscopy measurements were taken after each annealing period. Results showed that annealing produced no change in the Ba:Fe:As elemental ratio and did not lead to the inclusion of Tantalum.

3.1. Annealing induced changes in the magnetic susceptibility

In order to examine the effects of annealing on the magnetic properties of BaFe_2As_2 , magnetic susceptibility measurements were taken on a single crystal sample as grown and after each annealing period. Figure 1(a) shows these measurements across the phase transition(s), where the results have been normalized to allow for an easy comparison. The figure shows a step in the magnetic susceptibility that is indicative of a phase transition(s). Annealing raises the temperature of the phase transition(s) from 135.3 K in the as grown sample to 139.8 K after 46 d of annealing. The transition temperature(s) for the sample after 46 d of annealing is slightly lower than the value previously reported in a 30 d annealed sample (140.2 K) [18]. However the important point is that post growth annealing raises the temperature of the phase

transition(s) in BaFe_2As_2 . To further investigate the effects of annealing on the nature of the phase transition(s), we have plotted $\partial(\chi T)/\partial(T)$ in figure 1(b). $\partial(\chi T)/\partial(T)$ is known to mimic the heat capacity of both the magnetic and structural phase transitions in the 122 compounds [21, 23]. Thus we are able to make an approximate comparison to our previous heat capacity measurements [18], however the establishment of a precise quantitative comparison between these two sets of measurements is beyond the purpose of this study. Like our previous heat capacity measurements, figure 1(b) shows that annealing for long periods causes the peak in $\partial(\chi T)/\partial(T)$ to sharpen. Similar magnetic susceptibility measurements taken on $\text{Ba}(\text{Fe}_{1-x}\text{Co}_x)_2\text{As}_2$ show that the main peak in $\partial(\chi T)/\partial(T)$ arises from the magnetic phase transition, while a shoulder on the high temperature side of the peak represents the structural phase transition [21, 23]. Our susceptibility data appear as a single peak for all annealing periods, indicating the absence of a distinguishable shoulder feature that would correspond to the structural transition. Therefore it is likely that the peak in figure 1(b) corresponds to the first-order magnetic phase transition. However if the structural transition does contribute to the weight of the susceptibility anomaly, as is the case in lightly cobalt-substituted samples [21, 23], then the sharpening of the anomaly is not inconsistent with the results of our x-ray diffraction measurements, namely that the separation between the magnetic and structural transition temperatures decreases with annealing until they converge.

3.2. Annealing induced changes in the c -axis lattice parameter

An investigation into the variations of the lattice parameters might provide useful information into how the process of annealing is modifying this material, and also serve as a benchmark to compare sample quality across studies. To this end, room temperature x-ray diffraction measurements of the out-of-plane reflections: (0 0 4), (0 0 8) and (0 0 12), were taken in the same single crystal, as grown and after each annealing period. Figure 2 shows longitudinal scans across the (0 0 8) reflection for the different annealing periods. The reflections were fitted using a non-linear least squares analysis with a Gaussian function. This fit profile was chosen because it gave a better agreement to the data than a Lorentzian or Lorentzian-squared profile. The figure shows that annealing has three effects. First, it causes the reflection's intensity to decrease; this may be linked to the crystal becoming duller and/or an increase in crystal's mosaic spread with annealing (see section 2). Second, annealing periods of less than or equal to 30 d cause the 2θ angle of reflection to increase, revealing that the c -axis lattice parameter contracts. Although it should be noted that this reduction in the c -axis is quite small. Comparing annealing periods of 30 and 46 d, the reflection's position remains unchanged. These observations also hold true for the (0 0 4) and (0 0 12) reflections. This result is summarized in table 1, which gives the c -axis lattice parameter as determined from the mean value of the positions of the three out-of-plane reflections. Finally, annealing causes a reduction in the width of these reflections. For example the FWHM extracted from

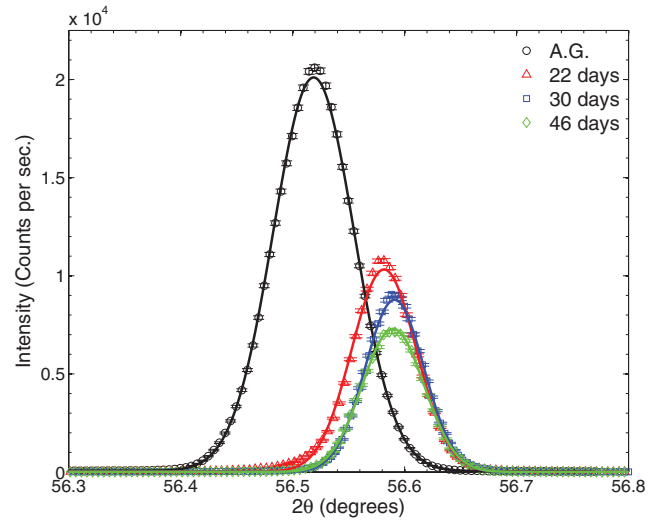


Figure 2. Longitudinal scans of the BaFe_2As_2 (0 0 8) reflection for as grown (A.G.) and after 22, 30 and 46 d of annealing. The reflections are fitted with a Gaussian profile.

Table 1. The c -axis lattice parameter and errors for the various annealing periods. These values were determined from fitting the (0 0 4), (0 0 8) & (0 0 12) reflections with a Gaussian curve and taking the mean value.

Annealing time (days)	c -axis lattice parameter (\AA)
0	$13.0168 \pm 9 \times 10^{-4}$
22	$13.0039 \pm 1.9 \times 10^{-3}$
30	$13.0024 \pm 1.3 \times 10^{-3}$
46	$13.0025 \pm 1.9 \times 10^{-3}$

Note: For examples of the Gaussian fits see figure 2.

the Gaussian fit of the (0 0 8) was reduced from $8.53 \times 10^{-2}^\circ$ as grown to $6.51 \times 10^{-2}^\circ$ after 46 d of annealing. The reduction in FWHM of these reflections indicates an increase of the correlation length, thus suggesting that annealing causes an improvement of the sample's crystallinity. However the intrinsic diffraction profile of a Bragg reflection is normally Lorentzian in nature. Therefore the Gaussian profile that we see in our measurements indicates that there are other significant factors, such as the diffractometer's resolution function, that affect the peak's shape. As such it is difficult to make a definite conclusion as to the reason for this reduction in width.

3.3. Annealing induced changes as seen with x-ray measurements of the structural phase transition

The final part of this section will focus on any annealing induced changes in the coupling of the structure to the magnetism. In order to study this, we have performed high resolution synchrotron x-ray diffraction measurements of the tetragonal to orthorhombic structural phase transition in as grown, and after 30 and 46 d of annealing. Since the second to first-order jump in the structural phase transition is due to the on-set of the antiferromagnetic order [20], these x-ray diffraction measurements should provide information on subtle changes in

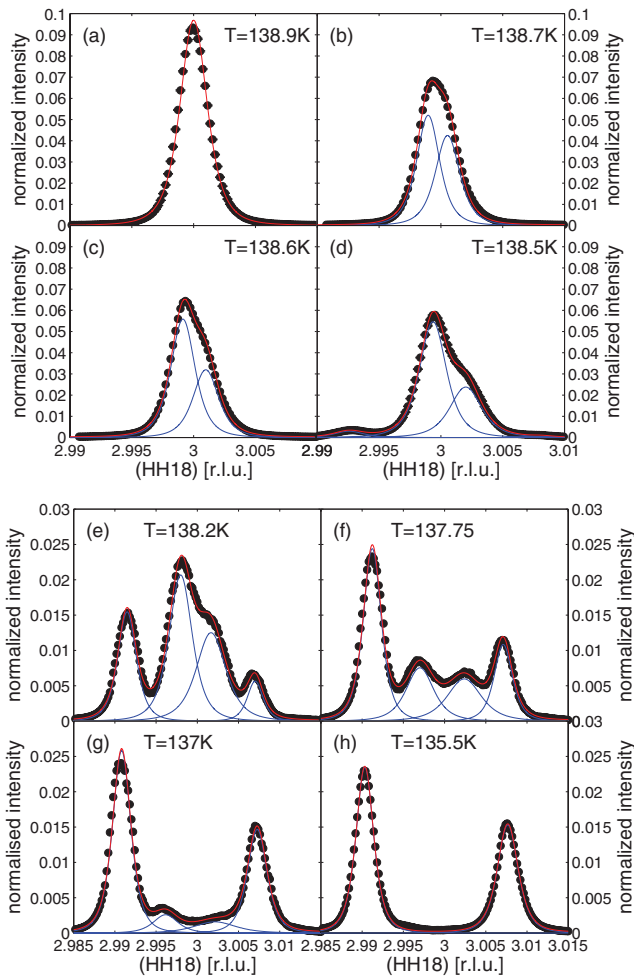


Figure 3. Examples of reciprocal lattice scans across the $(3\ 3\ 18)_T$ reflection in the BaFe_2As_2 single crystal after 30 d annealing. All peaks are fitted with a Lorentzian squared profile.

the nature, temperature and coupling of the structural and magnetic phase transition.

Measurements taken on the sample as grown and after 30 d of annealing both exhibit the now familiar structural phase transition: upon cooling the tetragonal reflection broadens and then splits. At a slightly lower temperature, a second set of (outer) reflections suddenly appears. The positions of these outer reflections are only weakly temperature dependent, although their intensity increases with decreasing temperature. Upon a further decrease in temperature the first set of reflections is rapidly suppressed, while their positions continue to separate, they never merge with the second set of reflections. An example of this phase transition is given in figure 3, which shows the $(3\ 3\ 18)_T$ tetragonal reflection splitting into the $(6\ 0\ 18)_O$ and $(0\ 6\ 18)_O$ orthorhombic reflections. These measurements were taken on the sample after 30 d of annealing.

By contrast the structural phase transition after 46 d of annealing appears to be purely first-order to at least 0.1 K. This result is given in figure 4, which shows the evolution of the $(2\ 2\ 16)_T$ tetragonal reflection into the $(4\ 0\ 16)_O$ and $(0\ 4\ 16)_O$ orthorhombic reflections upon cooling. Here the continuous splitting of the tetragonal reflection was not observed, instead a set of first-order orthorhombic reflections appear

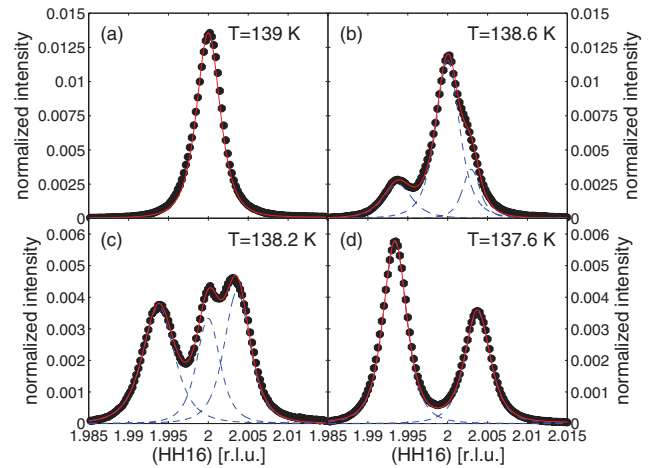


Figure 4. Examples of reciprocal lattice scans across the $(2\ 2\ 16)_T$ reflection in the BaFe_2As_2 single crystal after 46 d of annealing. All peaks are fitted with a Lorentzian squared profile.

Table 2. Characteristic temperatures of the structural phase transition in as grown, 30 & 46 d annealed BaFe_2As_2 , measured upon cooling.

Annealing time (days)	T_S (K)	T_N (K)	$T_S - T_N$ (K)	ΔT_S (K)
0	134.6 [135.2]	133.8	0.8 [1.4]	1.8
30	138.8 [139.5]	138.5	0.3 [1.0]	1.5
46	138.7	138.7	0	0.8

Note: Here T_S is the temperature where the continuous splitting of the tetragonal reflection is first detected. The value in the square brackets is the temperature where the broadening of this reflection is first detected. T_N is the temperature where the continuous splitting of tetragonal reflection is interrupted by the appearance of the second set of orthorhombic reflections. $T_S - T_N$ is the difference in temperature between the first appearance of the continuous splitting of tetragonal reflection and the appearance of the second set of orthorhombic reflections. The value in square brackets is the difference between the initial broadening of the tetragonal reflection and the appearance of the second set of orthorhombic reflections. Finally, ΔT_S is the difference in temperature between T_N and the disappearance of the inner set peaks (as grown and 30 d annealed), or the tetragonal peak (46 d annealed).

abruptly at 138.7 K (for example see figure 4(b)). Upon a further decrease in temperature, the intensity of these reflections increase but their position remains approximately constant. Simultaneously, the intensity of the tetragonal reflection decreased, but no significant change in position or width of this reflection was detected. It should be noted that the value for T_S is slightly less in the sample after 46 d of annealing than after 30 d of annealing (see table 2). However this disparity is small and likely due to a difference in the thermal contact between the sample and cold finger on the two occasions the sample was measured.

To emphasize the effects of different annealing times, we have plotted the structural order parameter: $\delta = (a_o - b_o)/(a_o + b_o)$, close to the phase transition in figure 5(a). Figure 5(b) displays the FWHM of fits to the tetragonal reflection for temperatures just above structural phase transition in the sample as grown and after 30 d of annealing. For comparison, the structural order parameter of as grown SrFe_2As_2 is plotted in figure 6. These measurements

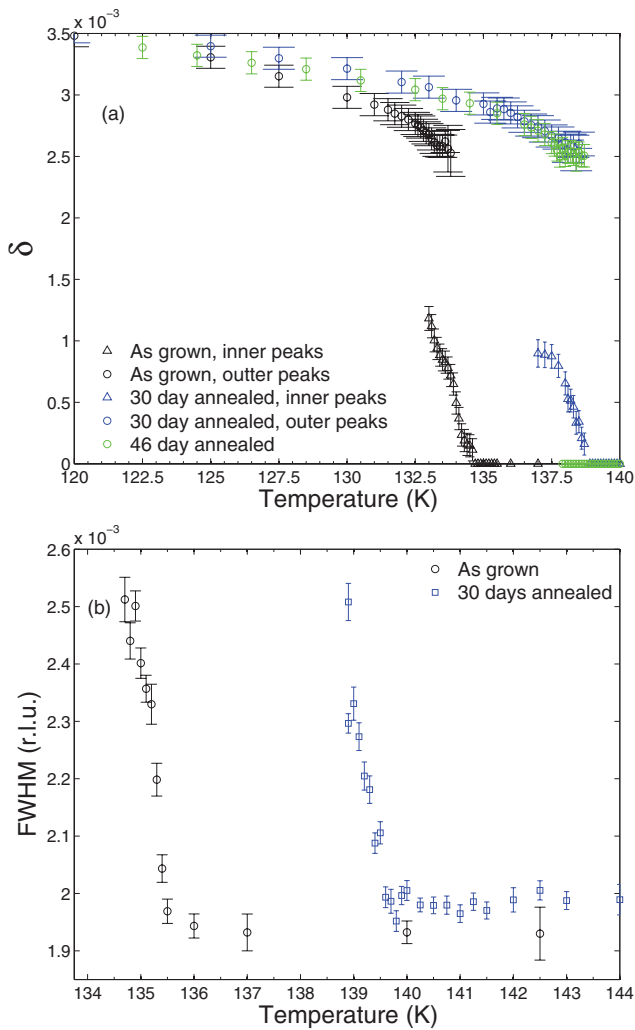


Figure 5. (a) The BaFe₂As₂ structural order parameter: $\delta = (a_0 - b_0)/(a_0 + b_0)$ versus temperature for as grown, and after 30 and 46 d of annealing. (b) The FWHM of the (3 3 18)_T reflection in the sample as grown and after 30 d of annealing samples. Results show that upon cooling, there is a broadening of this reflection for temperatures just above the structural phase transition.

were taken under the same experimental conditions as for BaFe₂As₂. The figure shows that the structural phase transition is first-order in SrFe₂As₂ and similar in nature to BaFe₂As₂ after 46 d of annealing. Therefore it seems that the structural phase transition in as grown BaFe₂As₂ is unique in the 122 parent compounds [13, 14].

It is important to note that annealing does not cause a change in the final value of δ (see figure 5(a)). Thus annealing does not affect the final orthorhombic distortion, just its onset temperature. In addition, the study by Kim *et al* [20] has shown that the jump in the structural order parameter corresponds to the onset of the antiferromagnetic order. Therefore the difference between the temperature of the initial splitting of the tetragonal reflection, and the appearance of the second set of orthorhombic reflections, can be interpreted as the difference between the structural and magnetic phase transition temperatures, this is shown the third column in table 2. Initially the difference between ordering temperatures is 0.8 K, or 1.4 K if one defines the broadening of the tetragonal

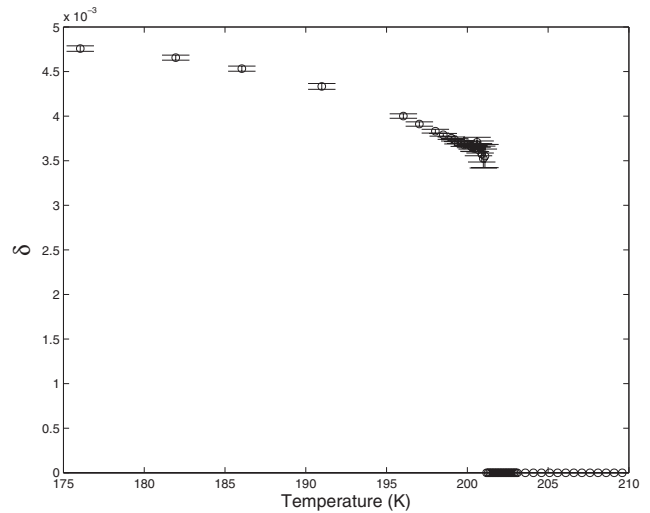


Figure 6. The structural order parameter of as grown SrFe₂As₂, measured under the same experimental conditions as the order parameters shown in figure 5(a).

reflection as the start of the structural phase transition. After 30 d of annealing, the difference in ordering temperatures is reduced to 0.3 K, or 1 K if again one includes the broadening of the tetragonal reflection. Because the structural phase transition after 46 d of annealing is completely first-order, we believe that annealing for this length of time causes the magnetic and structural ordering temperatures to converge to within at least 0.1 K. It is also worth mentioning that the temperature range of coexistence between the two sets of reflections, shown in the fourth column of table 2, decreases with annealing time. For example, the inner and outer peaks coexist in the as grown sample over a range of 1.8 K, but the corresponding value in the sample after 46 d of annealing is reduced to 0.8 K.

At this point it should be noted that the ordering temperatures given in table 2 are slightly lower than the ordering temperatures indicated by the magnetic susceptibility (figure 1). Likely explanations for this inconsistency include slight differences in the calibrations of the respective thermometers, and their distance to the sample. The main point, however, is that like the magnetic susceptibility measurements, these x-ray measurements show that annealing increases the ordering temperatures of the phase transitions. Thus the changes in the transition temperatures with annealing observed in our study, and the character of the structural order parameter in the sample as grown and after 30 d of annealing, are consistent with the previous studies [18, 20].

4. Discussion

We have shown that annealing of BaFe₂As₂ at 700 °C over an extended period of time causes the structural and magnetic phase transitions to increase and converge in temperature. This culminates after 46 d of annealing where the two phase transitions are coincident in temperature to at least 0.1 K. The present study also confirms that the two phase transitions are separated in temperature in as grown samples, which did not involve a decanting step in the crystal growth process [20].

In contrast, the structural phase transition in as grown SrFe_2As_2 is purely first-order in nature, indicating that the two phase transitions are concurrent in the compound. Therefore the separation in temperature of the two phase transition is likely to be intrinsic and unique to as grown BaFe_2As_2 , and thus the effects of annealing may also be unique.

It has already been demonstrated that the magnetic transition is first-order in the parent compound, but crosses over to second-order at a tricritical point as a function of chemical substitution [20, 21]. Here we have the result that the structural transition is first-order for the long-time (46 d) annealed sample, but is second-order in either as grown samples or with shorter annealing times. Therefore it seems that the structural phase transition line also has a tricritical point, albeit one which arises from the strong magnetoelastic coupling to the magnetic phase transition. As we have stated in section 1, this result was predicted by mean-field calculations as a consequence of a reduction in the bare shear modulus [20]. Thus this result can be explained by annealing inducing changes in the elastic properties of BaFe_2As_2 , without the need to change the strength of the magnetoelastic coupling. This argument is supported by the fact that annealing does not change the size of the orthorhombic distortion (δ).

We now return to the question of the effect of annealing at the microscopic level in BaFe_2As_2 . The simplest scenario is that annealing modifies the concentration of a certain defect species, such as site disorder, dislocations, vacancies or interstitial species, which mimic the effects of chemical substitution. It is not unreasonable to postulate that such impurities may have a similar effect on the elastic properties of BaFe_2As_2 to that of low levels of chemical substitution, for example lightly doped $\text{Ba}(\text{Fe}_{1-x}\text{Co}_x)_2\text{As}_2$. This explanation is supported by the improved crystalline quality of long timed annealed BaFe_2As_2 crystals, as shown by our previous measurements which give an increase in the RRR values with annealing [18], and our current measurements which show the reduction in the temperature range of coexistence between the two set of orthorhombic reflections (the final column in table 2), and the reduction in FWHM of the (0 0 L) reflections as shown in section 3.2. In addition, for a first-order phase transformation, the suppression of the phase transition temperature is a hallmark of quenched disorder: the transition temperature of a first-order transition is suppressed in the presence of disorder due to the finite energy of forming domain walls [24]. Thus the increase of T_N could be taken as evidence that, at the least, the disorder is homogenized in annealed samples. Even slight amounts of disorder can cause the phase transition to round, and lower the latent heat of the transition. Therefore the increase and sharpening of the magnetic phase transition with annealing (see section 3.1 and [18]), could be explained by the removal of defects.

Another possibility is that oxygen or water is introduced to the system by repeated annealing and exposure to the ambient environment during the course of the x-ray and susceptibility measurements. However this hypothesis seems to be at odds with published research. For instance, the absorption of oxygen in BaFe_2As_2 has been shown to suppress T_S and/or T_N , and cause these phase transitions to round [25]. This

result, combined with the fact the tantalum is a well-known getter, indicates that such impurities are not being introduced by the annealing process. Although studies of the effects of annealing without tantalum would provide further insight on this issue. Although we cannot specify the types of defects and impurities present in our samples, we suggest that their elimination by annealing may correlate with the trends described in this paper.

Another possible mechanism which may be responsible for the evolution of T_S and T_N involves reorientation of the excess FeAs flux within the crystal; for $\text{Ca}(\text{Fe}_{1-x}\text{Co}_x)_2\text{As}_2$ [26, 27] it was suggested that nanoscale precipitates with compositions close to that of the flux effectively induce hydrostatic pressure on the quenched crystals. The solubility of the flux, and hence the effective pressure induced by the precipitates are then proportional to the temperature from which the crystals are quenched. If this model were applicable for BaFe_2As_2 , we would expect the annealing process to reduce the effective pressure on the crystals, since the annealing temperature (700 °C) is lower than that of the final reaction temperature of the as grown crystals (900 °C). Work by Saparov *et al* has suggested that annealing of BaFe_2As_2 and SrFe_2As_2 crystals does produce a pressure-like effect [28]. Specifically, resistivity measurements showed that annealing at 350 °C induces a larger increase in the transition temperatures, when compared to annealing at 700 °C. However it should be noted that this previous research was studying changes due to variations in the annealing temperature, whereas the research described here is studying changes due to the annealing period. Therefore the effects of the two annealing processes may not necessarily be the same.

While it is possible that annealing leads to a change in the effective pressure, the results we report here are inconsistent with studies in which an external pressure, either hydrostatic or uniaxial, is applied. In brief, an increase in hydrostatic or uniaxial pressure along the *c*-axis could explain the compression of the *c*-axis lattice parameter. However for both cases the increase in pressure leads to a suppression of T_S and T_N [29, 30]. By contrast, the application of compressive or tensile stress within the *ab*-plane does cause an increase in T_S , however it also causes the structural transition to smear in temperature [31, 32]. This is the opposite to what we observe with annealing; either the stress is increased and both T_S and the smearing are increased, or the stress is reduced and T_S decreases with the structural transition becoming sharper. Even so, additional studies into the effects of annealing on BaFe_2As_2 crystals that have been decanted from their FeAs flux would provide a useful insight.

5. Conclusions

In conclusion, we have studied the effects of post growth annealing on the structural and magnetic properties of the pnictide BaFe_2As_2 . Our results show that annealing at 700 °C causes the ordering temperatures of both the structural and magnetic phase transitions to increase and converge, culminating in 46 d of annealing where they are coincident to less than 0.1 K.

Thus the 46 d annealed BaFe₂As₂ undergoes a single first-order phase transition from a tetragonal-paramagnetic phase to a orthorhombic-antiferromagnetic phase, without the transition to the intermediate orthorhombic-paramagnetic phase. Therefore annealing for long periods of time causes the system to cross a hitherto undiscovered tricritical point. This result can be explained by a change in the sample's elastic properties [20]. We argue that the hypothesis of annealing-induced changes in the defect/dopant densities, provides the best explanation of the experimental results presented in this paper and elsewhere [18], and therefore is the most likely method by which annealing changes the elastic properties of BaFe₂As₂. Finally, we argue that the phase diagram in the immediate vicinity of the pure system's tricritical point requires further investigation, both experimental and theoretical.

Acknowledgments

We thank S Mulcahy, J Heron, R Marks and V Borzenets for their assistance. This work was supported by the US Department of Energy, Office of Basic Energy Sciences, Materials Sciences and Engineering Division, under Contract No. DE-AC02-05CH11231. Portions of this research were carried out at the Stanford Synchrotron Radiation Lightsource, a Directorate of SLAC National Accelerator Laboratory and an Office of Science User Facility operated for the US Department of Energy Office of Science by Stanford University.

References

- [1] Kamihara Y, Watanabe T, Hirano M and Hosono H 2008 *J. Am. Chem. Soc.* **130** 3296–7
- [2] Rotter M, Tegel M and Johrendt D 2008 *Phys. Rev. Lett.* **101** 107006
- [3] Tapp J, Tang Z, Lv B, Sasmal K, Lorenz B, Chu P and Guloy A 2008 *Phys. Rev. B* **78** 060505
- [4] Zhu X, Han F, Mu G, Cheng P, Shen B, Zeng B and Wen H H 2009 *Phys. Rev. B* **79** 220512
- [5] Sefat A, Jin R, McGuire M, Sales B, Singh D and Mandrus D 2008 *Phys. Rev. Lett.* **101** 117004
- [6] Leithe-Jasper A, Schnelle W, Geibel C and Rosner H 2008 *Phys. Rev. Lett.* **101** 207004
- [7] Li L *et al* 2009 *New J. Phys.* **11** 025008
- [8] Sasmal K, Lv B, Lorenz B, Guloy A, Chen F, Xue Y Y and Chu C W 2008 *Phys. Rev. Lett.* **101** 107007
- [9] Jiang S, Xing H, Xuan G, Wang C, Ren Z, Feng C, Dai J, Xu Z and Cao G 2009 *J. Phys.: Condens. Matter.* **21** 382203
- [10] Torikachvili M, Bud'ko S, Ni N and Canfield P 2008 *Phys. Rev. Lett.* **101** 057006
- [11] Alireza P, Ko Y, Gillett J, Petrone C, Cole J, Lonzarich G and Sebastian S 2009 *J. Phys.: Condens. Matter.* **21** 012208
- [12] Engelmann J *et al* 2013 *Nat. Commun.* **4** 2877
- [13] Ni N, Nandi S, Kreyssig A, Goldman A I, Mun E D, Bud'ko S L and Canfield P C 2008 *Phys. Rev. B* **78** 014523
- [14] Goldman A I, Argyriou D N, Ouladdiaf B, Chatterji T, Kreyssig A, Nandi S, Ni N, Bud'ko S L, Canfield P C and McQueeney R J 2008 *Phys. Rev. B* **78** 100506
- [15] Li H, Tian W, Zarestky J, Kreyssig A, Ni N, Bud'ko S, Canfield P, Goldman A, McQueeney R and Vaknin D 2009 *Phys. Rev. B* **80** 054407
- [16] Kofu M, Qiu Y, Bao W, Lee S H, Chang S, Wu T, Wu G and Chen X 2009 *New J. Phys.* **11** 055001
- [17] Wilson S D, Yamani Z, Rotundu C R, Freelon B, Bourret-Courchesne E and Birgeneau R J 2009 *Phys. Rev. B* **79** 184519
- [18] Rotundu C R *et al* 2010 *Phys. Rev. B* **82** 144525
- [19] Ishida S *et al* 2011 *Phys. Rev. B* **84** 184514
- [20] Kim M G, Fernandes R M, Kreyssig A, Kim J W, Thaler A, Bud'ko S L, Canfield P C, McQueeney R J, Schmalian J and Goldman A I 2011 *Phys. Rev. B* **83** 134522
- [21] Rotundu C R and Birgeneau R J 2011 *Phys. Rev. B* **84** 092501
- [22] Wang X F, Wu T, Wu G, Chen H, Xie Y L, Ying J J, Yan Y J, Liu R H and Chen X H 2009 *Phys. Rev. Lett.* **102** 117005
- [23] Chu J H, Analytis J G, Kucharczyk C and Fisher I R 2009 *Phys. Rev. B* **79** 014506
- [24] Imry Y and Wortis M 1979 *Phys. Rev. B* **19** 3580–5
- [25] Ghosh N and Raj S 2015 *AIP Conf. Proc.* **1665** 100009
- [26] Ran S *et al* 2011 *Phys. Rev. B* **83** 144517
- [27] Ran S, Bud'ko S L, Straszheim W E, Soh J, Kim M G, Kreyssig A, Goldman A I and Canfield P C 2012 *Phys. Rev. B* **85** 224528
- [28] Saparov B and Sefat A 2014 *Dalton Trans.* **43** 14971–5
- [29] Eguchi N, Kodama M, Ishikawa F, Nakayama A, Ohmura A, Yamada Y and Nakano S 2012 *J. Phys.: Conf. Ser.* **400** 022017
- [30] Yamazaki T, Takeshita N, Kobayashi R, Fukazawa H, Kohori Y, Kihou K, Lee C H, Kito H, Iyo A and Eisaki H 2010 *Phys. Rev. B* **81** 224511
- [31] Dhital C, Yamani Z, Tian W, Zeretsky J, Sefat A S, Wang Z, Birgeneau R J and Wilson S D 2012 *Phys. Rev. Lett.* **108** 087001
- [32] Blomberg E C *et al* 2012 *Phys. Rev. B* **85** 144509